Part I

Fundamentals

Chapter 1

Characteristics of Microbubbles

Hideki Tsuge
Keio University, Tokyo 166-0004, Japan
htsuge@jcom.home.ne.jp

By comparing microbubbles (MBs) with millimeter- or centimeter-sized bubbles, the following characteristics of MBs are listed:

1. **Small bubble size**
   The size of MBs is generally μm order; it depends on the working field, that is, 10–40 μm for bioactivity field and less than 100 μm for fluid physics field.
2. **Slow rising velocity**
   The rising velocity of an MB depends on the physical properties of liquids. For MBs of 100 μm diameter, Re number ($=dU\rho/\mu$) is nearly 1, and its shape is spherical. Such MBs behave as fluid (clean) spheres or solid (unclean) spheres. By the experimental results of the MBs' rising velocity, both fluid and solid spherical behaviours were observed, while the rather many experimental results following the Stokes equation [Eq. (1.1)] applicable to solid spheres are reported[1].

$$U = \rho g d^2/18\,\mu, \tag{1.1}$$

Micro- and Nanobubbles: Fundamentals and Applications
Edited by Hideki Tsuge

ISBN 978-981-4463-10-2 (Hardcover), 978-981-4463-11-9 (eBook)
www.panstanford.com

where U is the rising velocity, ρ is the liquid density, g is the gravitational acceleration, d is the bubble diameter and μ is the liquid viscosity. For example, 10 μm MBs rise only 20 cm in 1 h.

3. **Decreasing friction drag**
   Friction drag of gas–liquid two-phase flow decreases with increasing MB volume fraction in vertical pipe flow [2]. Such experiments of decreasing friction drag are now verified by blowing MBs from the bottom of big ships [3].
4. **High pressure inside MBs (self-compression effect)**
   Using Young–Laplace equation (Eq. (1.2)), the pressure in a bubble (ΔP) whose diameter is d increases to that larger than the surrounding pressure due to the surface tension σ.

$$\Delta P = 4\sigma/d \tag{1.2}$$

   For example, the inner pressures of bubbles whose diameters are 1 μm and 100 nm are 3.87 and 29.7 atm, respectively, using Eq. (1.2) (surface tension of water at 20°C: 72.8 mN/m, the surrounding pressure of bubble is 1 atm). With decreasing bubble size, the pressure in the bubble increases. With decreasing bubble size, the partial pressure of dissolved gas component, that is, the driving force of dissolution, increases and the gas dissolves easily.
5. **Large interfacial area**
   Interfacial area of bubbles divided by volume A/V is obtained by Eq. (1.3). With decreasing bubble diameter d, A/V increases and contributes to gas dissolution fraction.

$$A/V = 6/d \tag{1.3}$$

6. **Large gas dissolution**
   Mass transfer rate from gas to liquid, or dissolving rate N (mol/s), is written by Eq. (1.4) when the gas phase mass transfer resistance is neglected.

$$N = k_L A(p - p^*)/H, \tag{1.4}$$

   where k_L is the liquid phase mass transfer coefficient (m/s), A is the bubble surface area (m^2), p is the partial pressure of dissolved component in bubble (Pa), p^* is the partial pressure of gas phase equilibrium with dissolved component in liquid (Pa) and H is the Henry constant ($p = HC$).

The liquid phase mass transfer coefficient k_L is written by Eq. (1.5) when Re < 1, and the rising velocity of spherical bubble follows Stokes law, where D_L is the gas diffusion coefficient in liquid phase, d is the bubble diameter and U is the bubble rising velocity [4].

$$k_L = \frac{D_L}{d}\left[1+\left(1+\frac{dU}{D_L}\right)^{1/3}\right] \tag{1.5}$$

When bubble diameter changes from 1 μm to 1 mm for oxygen–water system (oxygen diffusion coefficient $D_L = 2.60 \times 10^{-9}$ m^2/s in water), the liquid phase mass transfer coefficient k_L becomes 10^{-4}–10^{-3} m/s by Eq. (1.5). Mass transfer rate N is obtained by Eq. (1.4) using the data of k_L and bubble inner pressure. When a 1 mm bubble segregates into bubbles whose diameters are 10 μm and 100 nm, bubble numbers increase by 10^6 and 10^{12} times, respectively. When the surface area of the 1 mm bubble is defined as 1, the surface areas of 10 μm and 100 nm bubbles increase to 6×10^4 and 6×10^{10}, respectively. When the mass transfer rate of the 1 mm bubble during 1 mm rise is considered as 1, mass transfer rates of 10 μm and 100 nm bubbles become 10^8 and 10^{18}, respectively, due to the decrease in rising velocity. By using MBs, the dissolution rate increases rapidly.

7. **Dissolution and contraction**
   Ohnari describes the contraction of MB as follows [5]:
   For the swirling-type MB generator, the pressure at gas suction becomes 0.06 MPa less than the atmospheric pressure. MBs are formed under the combined pressure of atmospheric pressure and static pressure; they are pressurised by liquid and begin to contract. Due to high pressure and high temperature, contraction and dissolution of MBs take place. As shown in Fig. 1.1, a 20 μm MB contracts and under 10 μm, it contacts rapidly and disappears. On the other hand, MBs larger than 65 μm will expand further [6].
8. **Negatively charged surface of MB**
   Takahashi measured the surface potentials of MBs using the experimental set-up of electrophoresis cells shown in Fig. 1.2 [1]. MBs formed by the generator in the water

reservoir were introduced to the electrophoresis cell (1.0 mm thick, 23.0 mm high and 75.0 mm wide). A transfer switch was used to change the direction of the electric potential in the electrophoresis cell every 1 s. As MBs are charged negatively, MBs rise in a zigzag manner as shown in Fig. 1.3.

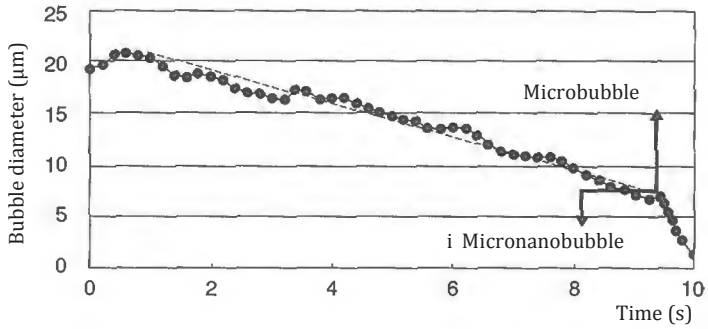

Figure 1.1 Time course of MB diameter.

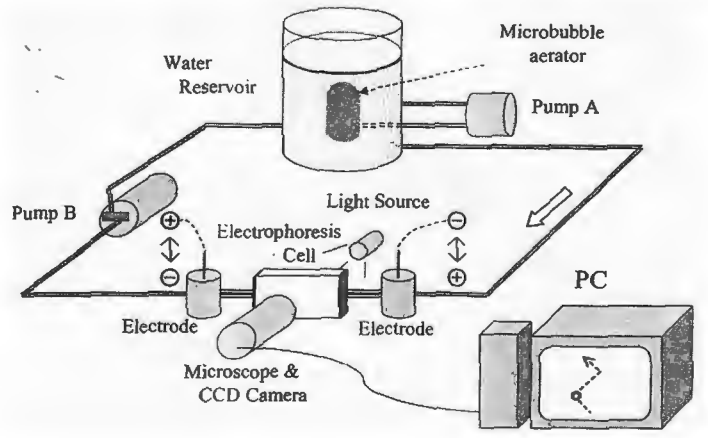

Figure 1.2 Experimental set-up of electrophoresis cell.

By measuring the vertical rising velocity of MBs, the bubble size is obtained using Stokes equation, and from the horizontal velocity, the ζ potential of MBs is obtained using Smoluchowski equation (Eq. (1.6)).

$$\varsigma = \mu u/\varepsilon, \tag{1.6}$$

where ζ is the zeta potential (V), μ is the viscosity of water (kg/ms), u is the mobility (m^2/sV) and ε is the permittivity of water (s^2C^2/kgm^3). Figure 1.4 shows the effect of bubble size on the ζ potential of MB in distilled water. MBs are negatively charged with an average ζ potential between –30 and –40 mV independent of bubble diameter.

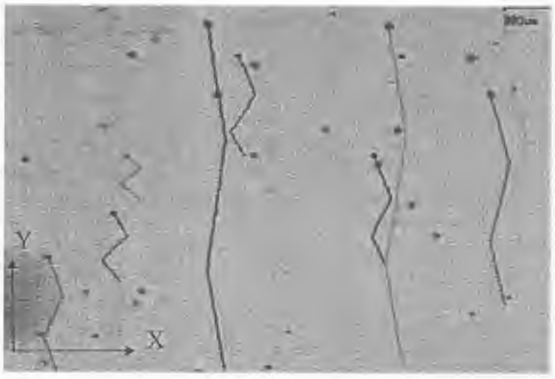

Figure 1.3 Rising loci of MBs.

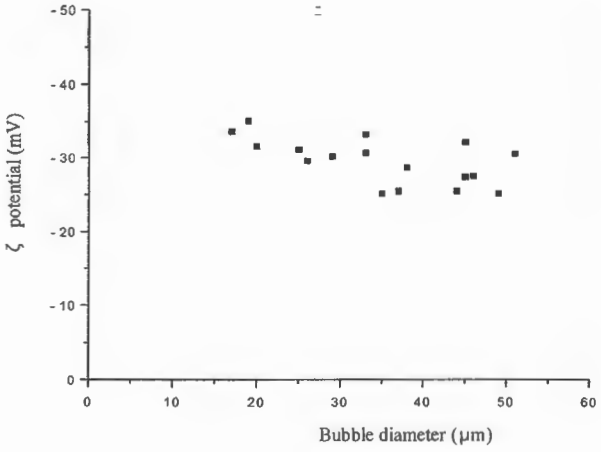

Figure 1.4 Effect of bubble diameter on ζ potential.

The gas–water interface is negatively charged; so, OH^- must play an important role in electrical charge. Takahashi explained the charging mechanism by using more

OH^- compared to H^+ ions at the gas-water interface [1]. Most researchers have explained the adsorption of OH^- onto the interface by the difference in hydrogen energy between H^+ and OH^- or by the orientation of water dipoles at the interface. Hydrogen atoms pointing towards the water phase and oxygen atoms towards the gas phase causes attraction of anions to the interface.

As shown in Fig. 1.5, the ζ potential of MB depends on the pH of the water adjusted by HCl and NaOH. The surface charge of the gas–water interface was strongly affected by the pH of the water. According to Takahashi, at strong acidic pH, ζ potential is 0 mV, while at strong base pH, it is –100 mV [1].

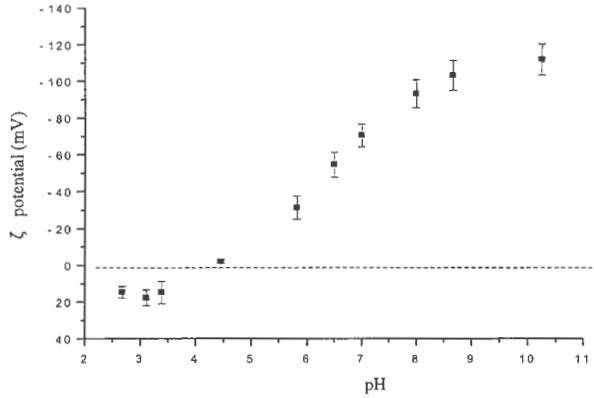

Figure 1.5 Effect of pH on ζ potential.

As the surface of MB is charged negatively, it shows that there is no possibility of coalescence of MB in the case of dense MB water. By charging the surface of suspended materials positively and adsorbing on the negatively charged surface of MB, we can apply it to the separation operation.

9. **Crushing and formation of free radicals**

Takahashi et al. introduced electrodes in water, crushing MBs by the shock waves formed and free radicals were created [7].

By comparing electron spin resonance, the number of formed free radicals by crushing shock waves on MBs

is two or three orders larger compared with the case of ultrasound radiation in water. Under 50 μm MB, free radicals are produced in several minutes during compression at high concentrations of MBs. As the ζ potential increases during compression, ion concentration around the MB increases so that excess ions are formed, and free radicals are created [7].

10. **Bioactivity effect**
    Ohnari observed growth promotion [5], shell opening and increase in rate of blood flow of oysters in Hiroshima, scallops in Hokkaido and pearls in Mie Prefecture, thus ascertaining the effect of bioactivity.

    Okajima and Harada observed the following medical findings [8]: by transcutaneous electrical nerve stimulation of MB, insulin-like growth factor-1 (IGF-1) was produced in living substances. By the stimulations of light and heat of MB, capsaicin-sensitive sensory nerves which detect temperature and pain are stimulated and calcitonin gene related peptide (CGRP) is released from the sensory nerves ends. As CGRP promoted the productions of NO and prostaglandin from vascular endothelial cells, IGF-1 is produced, and finally, increase in blood flow is promoted. The effect of MBs resembles the effect of capsaicin made using acidic hot springs and ginger extracts.
11. **Change of liquid properties by bubbling of MBs**
    Himuro found that by bubbling MBs in the city water at 25°C, liquid viscosity and surface tension decrease and electrical conductivity increases [9]. It is due to the change in cluster by cleavage of the hydrogen bond among water molecules and ionisation of chemicals in the city water.

References

1. Takahashi M (2005) ζ potential of microbubbles in aqueous solution: electrical properties of the gas-water interface, *J. Phys. Chem. B,* **109**, 21858–21864.
2. Serizawa A, Inui T, Eguchi T (2005) Flow characteristics and pseudo-laminarization of vertically upward air-water milky bubbly flow with micro bubbles in a pipe, *JJMF,* **19**, 335–343 (in Japanese).

3. Kodama Y (2007) Drag reduction of ship by microbubbles, *Chem. Eng. Jpn.,* **71**, 186–188 (in Japanese).
4. Clift R, Grace JR, Weber ME (1978) *Bubbles, Drops, and Particles*, Academic Press, New York.
5. Ohnari H (2007) Todays subjects of microbubble technology, *Chem. Eng. Jpn.,* **71**, 154–159 (in Japanese).
6. Ohnari H (2006) *All on Microbubbles*, Nippon Jitsugyo Shuppan Co., Japan (in Japanese).
7. Takahashi M, Chiba K, Li P (2007) Free-radical generation from collapsing microbubbles in the absence of a dynamic stimulus, *J. Phys. Chem. B,* **111**, 1343–1347.
8. Okajima K, Harada N (2007) Bioactivity of Microbubbles, in *The Latest Technology of Microbubbles and Nanobubbles*, CMC Book Co., Japan, 90–108 (in Japanese).
9. Himuro S (2007) Characteristics of physical chemistry of microbubbles, *Chem. Eng. Jpn.,* **71**, 165–169 (in Japanese).